Quantification of refractory gold in grains of pyrite and arsenopyrite from the "El Diamante" gold mine in Nariño - Colombia

Cuantificación de oro refractario en granos de pirita y arsenopirita de la mina de oro "El Diamante" en Nariño - Colombia

Bustos R. Humberto[I]; Dagoberto Oyola L. [I]; Rojas M. Yebrayl A. [I];
Pérez A. Germán A. [II]; Balogh Adam G. [III] and Cabri Louis J. [IV, V]

Abstract. Secondary Ion Mass Spectroscopy (SIMS) and Laser-Ablation Microprobe – Inductively Coupled Plasma – Mass Spectrometry (LAM–ICP-MS) techniques were used to study Colombian auriferous ores. The auriferous samples, collected from the El Diamante mine, located in Guachavez-Nariño (Colombia), were prepared as polished thin sections and polished sections. Petrographic analysis were made using an optical microscope with a digital camera, registering the presence, in different percentages, of the following phases: pyrite, quartz, arsenopyrite, sphalerite, chalcopyrite and galena. SIMS direct O_2^+ion images of ^{57}Fe, ^{34}S, ^{75}As and ^{197}Au were obtained from multiple regions with an approximately area of 200x200 μm in each sample.

The presence of refractory gold (invisible gold) associated mainly with pyrite and occasionally with arsenopyrite was recorded. LAM-ICP-MS results permitted quantification (in ppm) of invisible gold in multiple grains of arsenopyrite and pyrite and also to demonstrate that goldis present in variable concentrations as well as the As and Fe in these two structures. These results show that arsenic-rich pyrite is called arsenious pyrite [Fe(S, As)2].

I Departamento de Física, Universidad del Tolima, A. A. 546, Ibagué, Colombia
II Departamento de Física, Universidad del Valle, A. A. 25360, Cali, Colombia
III Institute of Materials Science, Darmstadt University of Technology, Germany
IV Cabri Consulting Inc., Ottawa, Ontario Canada
V Memorial University of Newfoundland, St. Johns, Newfoundland, Canada
hbustos@ut. edu. co

Key words: Invisible gold, secondary ions mass spectroscopy SIMS, LAM-ICP-MS, pyrite, quartz, arsenopyrite, ablation.

Resumen. Espectroscopia de masas de iones secundarios(SIMS) y espectrometría de masas de plasma acoplado inductivamente con microsonda de ablación láser(LAM-ICP-MS) se utilizaron como técnicas de estudio de menas auríferas colombianas. Las muestras auríferas, recolectadas de la mina El Diamante, ubicada en Guachavez-Nariño (Colombia), fueron preparadas como secciones delgadas pulidas y secciones pulidas. Los análisis petrográficos se realizaron con un microscopio óptico con cámara digital, registrando la presencia en diferentes porcentajes, de las siguientes fases: pirita, cuarzo, arsenopirita, esfalerita, calcopirita y galena. Imágenes SIMS directas de iones O_2^{+} de ^{57}Fe, 34S, 75 As y 197 Au se obtuvieron en varias regiones en un área de aproximadamente 200µx200µ en cada muestra. La presencia de oro refractario (oro invisible) asociado principalmente con la pirita y ocasionalmente con arsenopirita se registró. Resultados LAM-ICP-MS permite la cuantificación (en ppm) el oro invisible en varios granos de pirita y arsenopirita y también muestra que el oro está presente en concentraciones variables, así como el As y Fe en estas dos estructuras. Estos resultados muestran que la pirita es rica en arsénico, llamada piritaarseniosa [$Fe(S, As)_2$].

Palabras clave: Oro invisible, espectroscopia de masas de iones secundarios SIMS, LAM-ICP-MS, pirita, cuarzo, arsenopirita, ablación.

1. INTRODUCTION

Previous studies of the Diamante gold mine (Molano and J. Mojica 1998; Bustos Rodríguez *et al*., 2005, 2006, 2008), located in the municipality of Guachavez (Nariño)-Colombia, showed that this is a hydrothermal precious metal deposit mainly composed of quartz and approximately 30 % sulfides (pyrite, sphalerite and arsenopyrite).The gold in particular is associated firstly with pyrite and quartz and secondarily with arsenopyrite, sphalerite and galena. The composition of gold was determined by electron probe microanalysis (EPMA), indicating that this is electrum with 73% Au and 27% Ag.

The economic importance of gold has contributed to a significant increase in the exploration and study of these deposits. For most gold ores it is possible to recover up to ninety percent of gold by using conventional techniques such as gravity, flotation and cyanidation. However, the use of these and other techniques depend on many factors, such as: the mineral phase to which the gold is associated (visible or invisible), the type of gold present, the grain size, etc. (Harris, 1990). It is therefore important to obtain a good characterization of the mineralogical distribution of gold

ores to predict the best method of metallurgical recovery. The term "invisible" arises from the fact that one cannot distinguish, by conventional microscopy, between gold chemically bound in the mineral and submicroscopic inclusions (Cabri *et al.*, 2000). The question of the chemical form of "invisible" gold in sulfide and sulfarsenide minerals has also attracted much interest in the years that followed the first reports of chemically bound Au in sulfides (Marion *et al.*, 1986; Wagner *et al.*, 1986). The ore genesis and metallurgical implications of the presence of invisible gold in minerals such as arsenopyrite are potentially very significant (Mumin *et al.*, 1994), and experimental techniques to determine the valence of gold in sulfides and other minerals are also of current interest (Cabri *et al.*, 2000, Li *et al.*, 1995; Simon *et al.*, 1999; Wagner *et al.*, 1994). Experimental evidence, however, remains controversial because of low concentrations of gold, near the limits of resolution for conventional laboratory techniques, and its non-uniform distribution in sulfide minerals. Several analytical techniques have been developed to measure gold in pyrite and arsenopyrite such as secondary ion mass spectrometry (SIMS) (e.g., Cabri *et al.*, 1989; Chryssoulis *et al.*, 1989) or laser ablation microprobe inductively coupled mass spectrometry (LAM-ICP-MS) (e.g. Sylvester *et al.*, 2005).

Bombardment of a sample surface with a primary ion beam followed by mass spectrometry of the emitted secondary ions constitutes the SIMS technique. Today, SIMS is widely used for analysis of trace elements in solid materials, especially semiconductors and thin films. The SIMS ion source is operated most frequently with O or Cs ions. The SIMS primary ion beam can be focused to less than 1 μm in diameter. Controlling the point where the primary ion beam strikes the sample surface is the basis stage for the microanalysis process, the measurement of the lateral distribution of elements is done on a microscopic scale. During SIMS analysis, the sample surface is slowly sputtered away and continuously analysed while sputtering produces information as a function of depth (i.e., a depth profile). When the sputtering rate is extremely slow, the entire analysis can be performed while consuming less than a tenth of an atomic monolayer. This slow sputtering mode is called static SIMS in contrast to dynamic SIMS used for depth profiles. Shallow sputtering minimizes the damage done to organic substances present on the sample surface. The resulting ion fragmentation patterns contain useful information for identifying molecular species.

Laser ablation microprobe (LAM)-ICP-MS is firmly established as a fast, sensitive and reliable technique for *in situ* determination of trace elements in minerals and their inclusions. The technique couples the high resolution sampling capabilities of a pulsed UV laser with the extraordinary detection capabilities of the ICP-MS.

Current instrumentation is capable of simultaneously determining 30-40 elements in spots of 30-40 μm diameter at detection limits down to the ppb level for many elements. Minimal sample preparation is required and a typical analysis takes less than 2 minutes. Using the depth profiling capability of the laser, it is also possible to assess the homogeneity of the ablation volume and so determine whether elements are concentrated homogeneously in the lattice structure, or whether they are chemically zoned or occur in inclusions. The technique already has very useful isotopic applications (*e.g.*, U/Pb dating) and, with the recent advent of multi-collector ICP-MS instrumentation, an age of rapid, *in situ*, high precision isotope ratio analyses (*e.g.*, U/Pb, Re/Os, Sm/Nd, Lu/Hf, Rb/Sr) is dawning.

2. EXPERIMENTAL

Polished thin sections of 8 samples were prepared for petrographic analysis and were marked as sample numbers 805700, 805695, 805694, 805691, F2L1S1, PD14163, PD14163R and PD10114. The degree of reflectivity and anisotropy (if any) of each of the minerals present in the sample was used for identification using a polarization microscope with 5x, 10x, 20x, 50x, 100x objectives. Polished sections of 805700, 805694 and 805691 samples were prepared for the SIMS and LAM-ICP-MS analysis and also examined through by polarizing microscopy.

The SIMS ion images were obtained withdirect O_2^+ions for multiple regions of approximately 200 x 200 μm in area using a CAMECA ims 5f instrument with a primary ion current usually varying between 0.2 and 20 nA and the accelerating voltage of the primary ions was 12.5 keV with the effective voltage difference between ion source and sample being 8 keV (4.5 kV sample potential). However It was not possible to image with Cs primary ions (e.g., Steele *et al.*, 2000) at the time the samples were available. Because ^{32}S interferes with $^{16}O_2$, ^{34}S was used though it has lower abundance. Unfortunately, this ion, together with the low primary current used resulted in only a few bight pixels and some blue ones on a logarithmic scale.

For LAM-ICP-MS concentrations of the metals and metalloid elements Mg, Si, Ca, Ti, V, Cr, Fe, Co, Ni, Cu, Zn, Ga, As, Mo, Ag, Cd, Sn, Sb, Pb, and Bi were determined in addition to Au, the primary element of interest, at Memorial University of Newfoundland (MUN) using (LAM-ICP-MS). The analytical system is a Finnigan ELEMENT XR, a high resolution double focusing magnetic sector inductively coupled plasma mass spectrometer (HR-ICPMS), and a GEOLAS 193 nm excimer laser system. Ablations were performed in an argon-fluorine gas laser emitting at the 193

nm wavelength just prior to the feed to the torch. Nebulizer flow rates were 1.250 l/min He with an additional 0.56 l/min Ar make up gas added after the ablation cell. Laser energy was approximately 10 J/cm^2; a laser repetition rate of 10 Hz produced a ~ 40 μm diameter spot on the sample. Time resolved intensity data were acquired by peak-jumping in a combination of pulse-counting and analog modes, depending on signal strength, with one point measured per peak for masses 33 & 34 (S), 57 (Fe), 59 (Co), 65 (Cu), 75 (As), 107 & 109 (Ag), 121 (Sb), and 197 (Au). The internal standard element was S (using mass 33), whose concentration was assumed to be stoichiometric in the unknowns. Approximately 30 seconds of gas background data were collected prior to each 60 sec ablation of both standards and unknowns.

Standards used were a fused pyrrhotite standard (po689) and a pressed powdered sulfide for the other elements (MASS-1; Wilson *et al.*, 2002) were used for concentration calibrations. Standard po689 was considered to be more reliable than MASS-1 because of its both homogeneity and physical properties. The methodology employed an analytical sequence of two analyses of standard po689 and one of standard MASS-1, then analyses of 6 to 14 unknown pyrite/arsenopyrite/sphalerite particles were employed, closing with a repetition of the same standards in reverse order. Analyses of the standard po41 (Sylvester *et al.*, 2005) were also included for quality control purposes. The data were collected in four separate analytical sessions over two and half days. Data were reduced using MUN's in-house CONVERT and LAMTRACE spreadsheet programs, which employ procedures described by Longerich *et al.* (1996). The program was also used to subtract the gas background, apply the internal standard correction for instrument sensitivity drift during the analytical session, and perform calculations converting count rates into concentrations by reference to the synthetic sulfide standards. The error for the method is estimated to be better than 10% relative based on the reproducibility of results for various reference materials measured from day to day over several months in the MUN laboratory. Limits of detection were typically between 0.008 and 0.020 ppm for the lighter elements and as low as 0.002 ppm for the heavy element (Au).

3. RESULTS AND DISCUSSION

3.1 Petrographic analysis results

In general, the petrographic analysis of the samples of the Diamante mine shows that the principal minerals are mainly sulfides: pyrite (cubic FeS_2), sphalerite (cubic ZnS) and arsenopyrite (FeAsS). In the present investigation it was however found that pyrite is associated with arsenopyrite, and sometimes is associated with sphalerite, appearing as crystalline aggregates or isolated crystals. Arsenopyrite is commonly associated with

the sphalerite and occasionally associated with pyrite. Sphalerite appears occasionally in isolated polycrystalline aggregates and normally associated with arsenopyrite and with pyrite. Chalcopyrite ($CuFeS_2$) is frequently associated with pyrite, arsenopyrite, sphalerite and freibergite [$(Ag, Cu, Fe)_{12}(Sb, As)_4S_{13}$] is sometimes found isolated in quartz. Galena (PbS) is associated with pyrite, arsenopyrite and sphalerite, and its occurrence is sporadic. Marcasite (orthorhombic FeS_2) is found generally intergrown in pyrite, but its occurrence is very rare. It is generally associated with chalcopyrite, in accordance with the reported literature (Molano, and Mojica, 1998). Typical photomicrographs are shown in figure 1, in which samples 805691**,** 805700 and 805688 are illustrated. The association of pyrite with arsenopyrite, sphalerite, and quartz can be seen sighted.

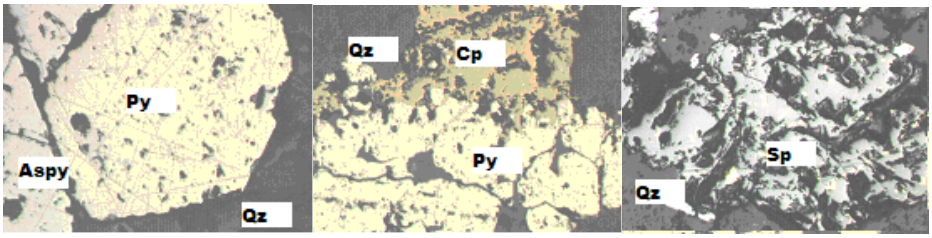

Fig. 1 Fig. 2 Fig. 3

Figures 1, 2 and 3. Photomicrographs of polished thin section (samples 805691, 805700 and 805688) using a magnification of 20x (Aspy, arsenopyrite; Py, pyrite; Qz, quartz; Sp, sphalerite; Cp, chalcopyrite).

3.2 Sims analysis results

Figure 4 shows SIMS ion images over an area of 200 x 200 μm of the sample 805694 for Fe, S, As and Au, respectively. The left side of the pictures corresponds to a region of an arsenopyrite grain and the small region of the right (one) corresponds to a pyrite, which has a small quantity of As, showing its arsenian character. It can be noticed that all four elements show zoning in the two phases, with a big abundance of As at left, Fe more or less uniformly distributed in the imaged area except in a zone starting at the top (middle) and then curves towards the right before curving left, which contains the highest intensity. Zones of most intense As and Fe (orange) are correlated and this can be due to a matrix effect produced by other surrounding elements which present also high signals (e.g. Cr, Si, K and Al, not showed here). The highest gold signal is registered inside of area of high content of As [As> Fe > S], and small quantities can be noted in the arsenian pyrite. Since the color scale is an indicative of the abundance, it can be noticed that the gold appears with variable concentration.

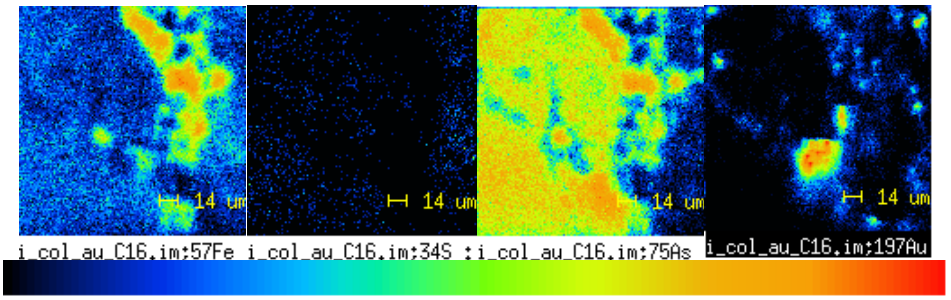

Figure 4. SIMS ion images on an area of 200 x 200 µm of sample 805694 (color scale indicates the abundance). In this case gold is associated with area of high content of Fe+As

Figure 5 shows the corresponding Au SIMS ion images for different parts of the same sample. They indicate that the gold presence is not uniform in this sample and in some places of it the Au may also occur as submicroscopic inclusions. All the pictures correspond to arsenian pyrite grains.This result was obtained for all the studied samples showing that, in general, gold appears more often in pyrite than in arsenopyrite. It can then be concluded that this type of invisible gold is preferentially associated with pyrite in samples from this gold auriferous mine.

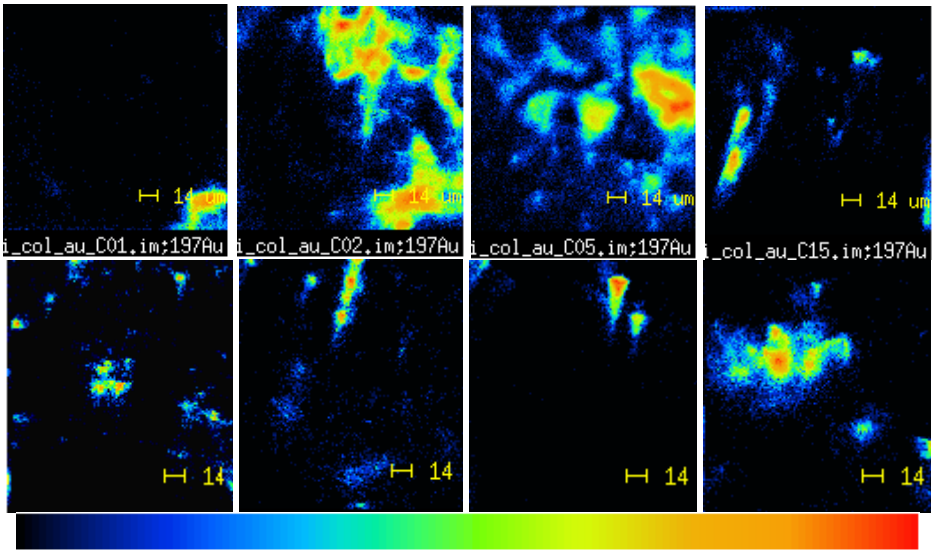

Figure 5. Au SIMS ion images for mineral sample 805694. All these are zones of arsenian pyrite (or maybe pyrite + arsenopyrite)

3.3 LAM-ICP-MS

Figures 6 to 11 show the profiles of the elements of interest as counts per second vs. time (s), obtained by the LAM-ICP-MS technique, in a single-spot ablations for pyrite and arsenopyrite in samples 805694, 805760 and 805691, respectively. It can be noticed that: in some of the samples the presence of Au is distributed almost homogeneously at the scale of the analysis and three or more orders of magnitude less counts than the other elements. Figure 10 shows Au zoning in pyrite as figure 11 does for arsenopyrite. In all the analyses high As counts were obtained, indicating that pyrite is arsenian pyrite. The detected total gold content obtained for the different spots of the samples shows, in general, that pyrite contains more Au than arsenopyrite (See table 1). However, in some spots Au counts for arsenopyrite are slightly higher than pyrite (see figures 6, 7, 8 and 9 for 805694 and 805700 samples). In general, the depth profiles of the elements, and particularly that of Au, do not show evidence of inclusions but suggest that the elements are chemically bound. However, Au and As in several spectra show evidence of zoning.

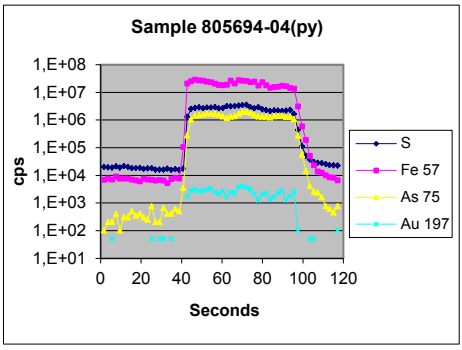

Fig. 6

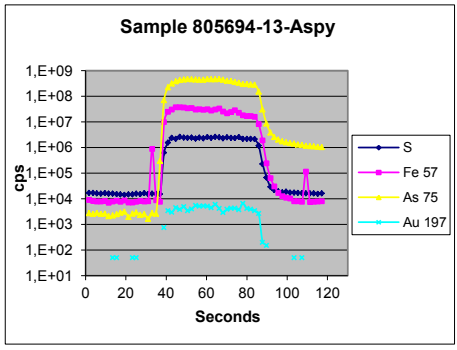

Fig. 7

The figures 6 and 7. Typical results recorded as counts per second (cps) *versus* time, obtained from single-spot ablation pits in the sulfide phases for pyrite (6) and arsenopyrite (7) of the 805694 sample.

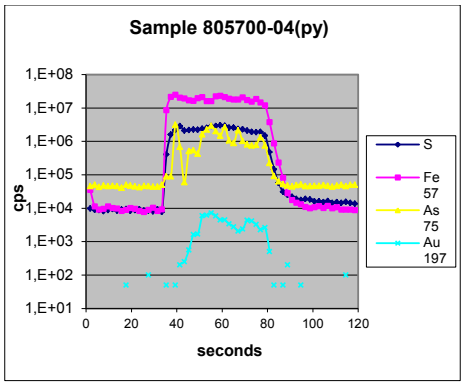

Fig. 8

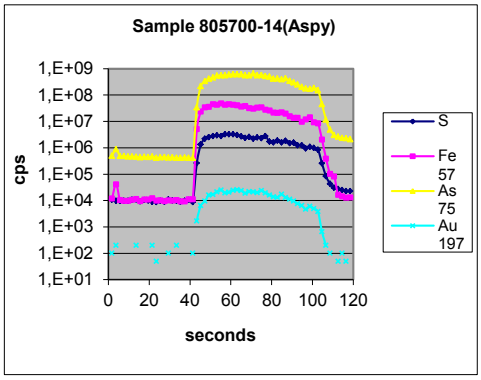

Fig. 9

The Figures 8 and 9. Typical results recorded as counts per second (cps) *versus* time, obtained from single-spot ablation pits in the sulfide phases for pyrite (8) and arsenopyrite (9) of the 805700 sample.

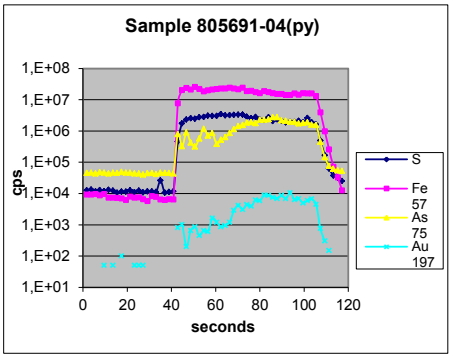

Fig. 10

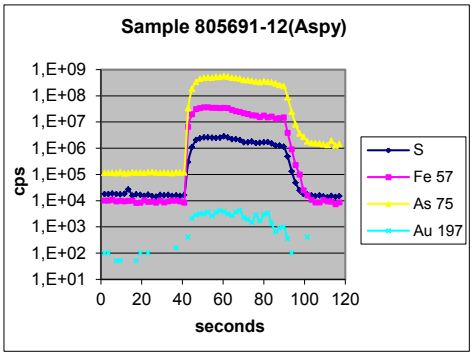

Fig. 11

Figure 10 and 11. Typical results recorded as counts per second (cps) *versus* time, obtained from single-spot ablation pits in the sulfide phases for pyrite (10) and arsenopyrite (11) of the 805691 sample.

Table 1 illustrates the complete results of the ablation experiments for the gold content of pyrite and arsenopyrite for these three samples.

Table 1. Ablation results (LAM-ICP-MS) for Au in pyrite and arsenopyrite

SPOT	SAMPLE 805700 (A)		SAMPLE 805691 (B)		SAMPLE 805694 (C)	
	Py (ppm)	Aspy (ppm)	Py (ppm)	Aspy (ppm)	Py (ppm)	Aspy (ppm)
1	5, 1058		6, 7740		3, 4450	
2	4, 6937		7, 0202		4, 2056	
3	0, 6062		4, 9973		10, 2457	
4	8, 9680		4, 5886		2, 2326	
5			18, 6578		5, 0531	
6			1, 6244		0, 3947	
7			2, 3237		2, 8310	
8			0, 6848		5, 6468	
9				2, 1305	18, 9805	
10				4, 6869		2, 5614
11		5, 4263		2, 4142		6, 6733
12		7, 1744		1, 0983		7, 4966
13				0, 7646		2, 0500
14		11, 7681		1, 4769		6, 0987

4. CONCLUSIONS

The present study about Colombian auriferous quartz vein mineralization from the Diamante mine, indicates that the samples are rich in sulfides and show the presence of invisible gold associated mainly with pyrite and secondarily with arsenopyrite. Minerals such as pyrite, arsenopyrite, and sphalerite were the most frequently detected phases with pyrite commonly associated with the arsenopyrite and sphalerite.

Data on counts per second (cps) *versus* time acquired by LAM–ICP–MS and those obtained by SIMS indicate that the "invisible gold" within the arsenopyriteand pyrite probably occurs in chemically bound formwith variable proportions in the structure due to zoning. The chemically bound "invisible" gold has a higher concentration in the arsenian pyrite than in the arsenopyrite.

ACKNOWLEDGEMENTS

We are thankful to the Central Research Committee of the University of Tolima and COLCIENCIAS, for financial support; to the GMTF of University of Valle, Colombia, where part of the experimental work was conducted; to the Institute for Materials Science of the Darmstadt University of Technology, Darmstadt, Germany, where the SIMS analysis of mineral samples and Memorial University of Newfoundland (MUN), Canada where LAM-ICP-MS analysis.

REFERENCES

Bustos Rodríguez, H., Rojas Martínez, Y.A, Oyola Lozano, D., Pérez Alcázar, G.A., Fajardo, M., Mojica, J. & Molano, J.C. (2005). Structural and Electronic Properties Study of Colombian Aurifer Soils by Mössbauer Spectroscopy and X-Ray Diffraction. *Hyperfine Interactions,* 161**,** 61-68.

Bustos Rodríguez, H., Oyola Lozano, D., Rojas Martínez, Y.A Pérez Alcázar, G.A., Balogh, A.G.(2006). Invisible gold in Colombian auriferous soils. *Hyperfine Interactions*, 166**,** 605-611.

Bustos Rodríguez, H., Oyola Lozano, D., Rojas Martínez, Y.A Pérez Alcázar, G.A., Balogh, A.G., Cabri L.J. (2008). Mineralogical analysis of auriferous ores from the El Diamante mine, Colombia. *Hyperfine Interactions*, 175, 195-206.

Cabri, L.J., Chryssoulis, S.L., De Villiers, J.P.R., Laflamme, J.H.G. & Buseck, P.R. (1989). The nature of "invisible" gold in arsenopyrite. *Can. Mineral,* 27, 353-362.

Cabri, L.J., Newville, M., Gordon, R.A., Crozier, E.D., Sutton, S.R., Mcmahon, G. & Jiang, D.T. (2000). Chemical speciation of gold in arsenopyrite. *Canadian Mineralogist*, 38, 1265-1281.

Chryssoulis, S.L., Cabri, L.J & Lennard, W. (1989). Calibration of the ion microprobe for quantitative trace precious metal analyses of ore minerals. *Econ. Geol.*, 84, 1684-1689.

Harris, D.C. (1990). The mineralogy of gold and its relevance to gold recoveries. *Mineral. Deposita*, 25, S3-S7.

Li, J., Fing, D., Qi, J. & Zhang, G., (1995). *Acta Geol.Sinica*, 69, 67-77

Longerich, H.P., Jackson, S.E. & Günther, D. (1996). Laser ablation – inductively coupled plasma mass spectrometric transient signal data acquisition and analyte concentration calculation. *J. Anal. At. Spectrom.,* 11, 899-904.

Marion, P., Regnard, J.R. & Wagner, F.E. (1986). Étude de l'état chimique de l'or dans des sulfures aurifères pas spectroscopie Mössbauer. C.R. Acad.Sci. Paris, 302, 571-574.

Molano, J.C. And Mojica, J. (1998). Identificación de Sulfuros, sulfosales de plata y oro en la Mina el Diamante (Nariño)-Colombia, mediante análisis SEM-EDAX, Seminario Internacional, eds. *Ingeominas-Jica*, Cali, Colombia, p.25.

Mumin, A.H., Fleet, M.E. & Chryssoulis, S.L. (1994). Gold mineralization in As rich mesothermal gold ores of the Bogosu-Prestea mining district of the Ashanti Gold Belt, Ghana: remobilization of "invisible" gold. *Mineral. Deposita,* 29, 445-460.

Simon, G., Huang, H., Penner-Hahn, J.E, Kesler, S.E. & Kao, L-S (1999). Oxidation state of gold and arsenic in gold-bearing arsenian pyrite. *Am. Mineral*, 84, 1071-1079.

Steele, I.M., Cabri, L.J., Gaspar, J.C., Mcmahon, G., Marquez, M.A. & Vasconcellos, M.A.Z. (2000). Comparative analysis of sulfides for gold using SXRF and SIMS. *Can. Mineral.,* 38, 1-10.

Wagner, F.E., Marion, P. & Regnard, J.R. (1986). Mössbauer study of the chemical state of gold in gold ores. S.Afr.Inst. *Mining Metall.*, Johannesburg, 2, 435-443.

Sylvester, P.J., Cabri, L.J., Tubrett, M.N., Mcmahon, G., Laflamme, J.H.G. & Peregoedova, A. (2005). Synthesis and evaluation of a fused pyrrhotite standard reference material for platinum group element and gold analysis by laser ablation-ICPMS. *10th International Platinum Symposium "Platinum-Group Elements – from Genesis to Beneficiation and Environmental Impact", Oulu, Finland, 8-11 August, 2005,* Abstract (Eds. T.O. Törmänen & T.T. Alapieti), 16-20.

Wagner, F.E., Sawicki, J.A., Friedl, J., Mandarino, J.A., Harris, D.C. & Cabri, L.J. (1994). ^{197}Au Mössbauer study of the gold-silver ditellurides sylvanite, krennerite and calaverite. *Can. Mineral.*, 32, 189-201.

Wilson, S.A., Ridley, W.I. & Koenig, A.E. (2002). Development of sulfide calibration standards for the laser ablation inductively coupled plasma mass spectrometry technique. *J. of Analytical Atomic Spectrometry*, 17, 406-409

Referencia	Fecha de recepción	Fecha de aprobación
Bustos R. Humberto; Dagoberto Oyola L. ; Rojas M. Yebrayl A. ; Pérez Alcázar Germán A. ; Balogh Adam G. and Cabri Louis J. Cuantificación de oro refractario en granos de pirita y arsenopirita de la mina de oro "El Diamante" en Nariño - Colombia Revista Tumbaga (2011), 6, 153-164	Día/mes/año 09/11/2010	Día/mes/año 14/07/2011